

RESEARCH COMMUNICATION

A novel immunoglobulin superfamily receptor (19A) related to CD2 is expressed on activated lymphocytes and promotes homotypic B-cell adhesion

John J. MURPHY*¹, Paul HOBBY†, Juan VILARINO-VARELA*, Benjamin BISHOP*, Panagiota IORDANIDOU*, Brian J. SUTTON† and John D. NORTON‡

*Infection and Immunity Research Group, Division of Life Sciences, King's College London, Franklin–Wilkins Building, 150 Stamford Street, London SE1 9NN, U.K., †The Randall Centre, King's College London, New Hunt's House, Guy's Campus, London SE1 1UL, U.K., and ‡Department of Biological Sciences, University of Essex, Colchester, Essex CO4 3SQ, U.K.

A novel lymphocyte-specific immunoglobulin superfamily protein (19A) has been cloned. The predicted 335-amino-acid sequence of 19A represents a Type 1 membrane protein with homology with the CD2 family of receptors. A molecular model of the two predicted extracellular immunoglobulin-like domains of 19A has been generated using the crystal structure of CD2 as a template. In isolated lymphocytes, expression of 19A

is induced by various activation stimuli, and enforced expression of the 19A gene promotes homotypic cell adhesion in a B-cell-line model. Collectively these data imply that the 19A protein plays a role in regulation of lymphocyte adhesion.

Key words: B-lymphocyte, cell activation, cell-surface receptor, CD2 family, early response gene.

INTRODUCTION

The CD2 family of immunoglobulin superfamily receptors includes a number of surface molecules that are involved in lymphocyte signalling and adhesion (reviewed in [1]). Examples of these include CD2 itself, CD48, CD58, 2B4, CD84/LY9 and the signalling lymphocyte activation molecule (SLAM). Recently, individual members of this family have been shown to play important roles in the regulation of the immune response. The SLAM receptor, for example, has been shown to regulate both T- and B-lymphocyte adhesion and is an important co-stimulatory receptor in the adaptive immune response [2,3]. CD2 family members have also been implicated in the regulation of natural killer (NK)-cell function [1]. Antibodies to the mouse 2B4 molecule can induce NK-cell lysis, granule release and interferon- γ production [4]. The ligand for 2B4 is CD48 [5,6], another CD2 family member, and, indeed, it is a feature of this immunoglobulin superfamily subset that their counter-receptors are often members of the same family or else they can bind homotypically, as has been reported for the SLAM molecule [2]. The importance of SLAM and 2B4 in NK and T-cell regulation and interaction is highlighted by the finding that mutations in the SLAM and 2B4-associated signalling adapter molecule ('SAP') are implicated as a causative factor in X-linked lymphoproliferative disease ('XLP') [7–9].

A feature shared by a number of regulators of lymphocyte function is that they are encoded by genes that are induced as 'delayed' early response genes (ERG) following stimulation through mitogenic/activation signalling pathways (reviewed in [10]). We have previously reported on the isolation and characterization of a panel of cDNA sequences represent-

ing 'anonymous' genes from primary human (monoclonal) B-lymphocytes stimulated with PMA [11]. Several of these have subsequently been found to play important roles in the functions of lymphocytes and also in cells of other lineages [10,12]. In the present paper we describe the characteristics of one of these 'anonymous' cDNA clones, termed '19A'. The predicted amino acid sequence of the 19A protein represents a novel surface-receptor-like molecule with homology with the CD2 family of cell-surface proteins. Enforced expression of the 19A gene promotes homotypic cell adhesion, implying that the 19A receptor, like many other members of the CD2 family, may play an important role in lymphocyte adhesion functions.

EXPERIMENTAL

Materials

PMA and phytohaemagglutinin (PHA) were purchased from Sigma Chemical Company (Poole, Dorset, U.K.). Human recombinant tumour necrosis factor- α (TNF α) was purchased from R & D Systems (Abingdon, Oxford, U.K.). F(ab')₂ goat anti- μ antibody was purchased from Cappel (Cochranville, PA, U.S.A.). Anti-(human CD3) and anti-(human CD20) monoclonal antibodies were purchased from Becton Dickinson (Cowley, Oxford, U.K.). The G28-5 anti-(human CD40)-producing hybridoma was obtained from the American Tissue Culture Collection (Manassas, VA, U.S.A.). RPMI 1640, foetal-calf serum (FCS) and penicillin/streptomycin were all obtained from Life Technologies (Paisley, Renfrewshire, Scotland, U.K.). A monoclonal antibody to a 19A-specific peptide (PLKSKVKQVDSI) was obtained from Eurogentec (Seraing, Belgium). The peptide epitope was identified from a corresponding region in CD2,

Abbreviations used: SLAM, signalling lymphocyte activation molecule; NK, natural killer; ERG, early response gene; EGFP, enhanced green fluorescent protein; FCS, foetal-calf serum; PHA, phytohaemagglutinin; B-CLL, B-cell chronic lymphocytic leukaemia; SCR, structurally conserved region; TNF α , tumour necrosis factor- α .

¹ To whom correspondence should be addressed (e-mail john.murphy@kcl.ac.uk).

The DNA sequence of the 19A-gene open reading frame, shown in Figure 1, has been deposited with the DDBJ, EMBL, GenBank® and GSDB Nucleotide Sequence databases under the accession number AJ276429.

previously shown to be recognized by a blocking anti-CD2 antibody [13].

Cloning and DNA sequencing of ERG 19A

The original 1.0 kb 19A cDNA was cloned and isolated as described previously from a cDNA library of B-cell chronic-lymphocytic-leukaemia (B-CLL) cells stimulated with PMA for 3 h [11]. Using the 19A cDNA as a probe, a longer cDNA of approx. 2.8 kb was isolated from a human peripheral-blood leucocyte cDNA library. DNA sequencing was carried out by the Molecular Biology Service Unit of King's College London.

Cell isolation and culture

Mononuclear-cell preparations were obtained from B-CLL patients with peripheral blood lymphocyte counts of less than 60×10^9 /litre. For isolation of peripheral-blood T-lymphocytes, buffy coats were obtained from the National Blood Service North London Centre, Colindale, London, U.K. Freshly excised tonsils were gently teased to release cells. Mononuclear cells were isolated by density-gradient centrifugation. B-cells and T-cells were purified with aminoethylthiuronium bromide-treated sheep red blood cells, followed by density-gradient centrifugation. All cell cultures (tonsillar B-lymphocytes, peripheral-blood T-lymphocytes and B-CLL cells) were purified to > 95% purity as judged by CD20 and CD3 staining and flow cytometry (results not shown). Cells were incubated in RPMI 1640 with 10% FCS, 2 mM glutamine and 100 µg/ml penicillin/streptomycin at 37 °C in a humidified incubator (5% CO₂ in air) for 16 h. Cells were then washed once and re-suspended at 1×10^6 viable cells/ml in tissue-culture flasks before addition of different agents.

Cell transfection and adhesion assay

The Daudi human B-cell line was transfected with 19A cDNA in the pcDNA3 mammalian expression vector. Cells were co-transfected with an enhanced green fluorescent protein (EGFP) containing plasmid. All transfections were carried out using an electroporator (Invitrogen, Carlsbad, CA, U.S.A.) at 250 V, 250 µF and infinite resistance. At 24 h after transfection, dead cells were removed from cultures by density-gradient centrifugation. In some experiments, anti-19A monoclonal antibody or an irrelevant antibody control was added to transfected cells after density-gradient centrifugation. After 48 h, cell adhesion was scored by counting adherent cells in the cultures using a fluorescent microscope (Leitz Dialux 20; Leica, Milton Keynes, U.K.). Clusters of two or more adherent cells were scored as positive and the percentages of adherent fluorescent and adherent non-fluorescent cells were scored in each of the cultures.

RNA hybridization analysis

Human B- and T-lymphocytes and B-CLL cells were harvested at various times after the addition of different agents as indicated in the text. Total RNA was isolated from cells by lysis in RNazol solution (Biogenesis, Poole, Dorset, U.K.) and purified according to the manufacturer's instructions. For B-CLL cells, 1.5 µg of RNA was dot-blotted on to nylon filter membrane (NEN Dupont, Boston, MA, U.S.A.) using a dot-blotting manifold (Schleicher und Schüll, Dassel, Germany) as described previously [11]. Alternatively, 2 µg RNA samples were electrophoresed through 1%-agarose gels in 0.8 M formaldehyde, and Northern blots were prepared as described previously [11]. Blots were hybridized with ³²P-labelled 19A cDNA probes and washed as

described previously [11]. In order to study the expression of 19A in different human cells and tissues, a ClonTech Human Multiple Tissue Array was hybridized to the ³²P-labelled 19A cDNA probe according to the manufacturer's instructions. The 19A cDNA probe was a 1 kb fragment in pUC9 [11].

Molecular modelling of 19A

The 19A sequence was analysed using the PSI-BLAST sequence analysis program at the National Center for Biotechnology Information website (<http://www.ncbi.nlm.nih.gov/>; see also [14]). For sequences showing only low similarity to proteins of known structure, fold-recognition algorithms can usefully provide confirmation of the structural fold, and suggest the most likely candidates among the crystal structure database for use as model templates. These include the algorithm 3-D PSSM [15] and THREADER [16], and both were used to determine the likely structural fold of 19A. Three-dimensional models of 19A were constructed using the molecular modelling programs INSIGHTII and HOMOLOGY (Molecular Simulations, Inc., Cambridge, U.K.) on a Silicon Graphics Indy workstation (Silicon Graphics Ltd., Reading, U.K.).

The 19A sequence was aligned with the sequence of template proteins according to the information provided by SCOP and BLAST and the fold-recognition programs. The extent of structurally conserved regions (SCRs) were carefully examined. Minor realignments were made to ensure correct positioning of conserved residues, paying particular attention to the disulphide-forming cysteine, and core hydrophobic, residues. Co-ordinates for the SCR of 19A were assigned directly from the template molecule.

Co-ordinates for external loop regions of 19A, which were not homologous with the template molecule, were obtained using the conformational search program GENLOOPS within the INSIGHT program suite. Loops were selected on the basis of acceptable stereochemical parameters: allowable phi and psi angles, the alignment of C_α-C_β bonds at splice points and, in particular, minimal steric interaction with adjacent loop or SCR residues. The whole model was then examined for steric overlaps, and these were relieved by replacing the existing side-chain rotamer with alternatives from the rotamer library in HOMOLOGY. Energy minimization was performed using AMBER. The structure was assessed using PROCHECK [17].

RESULTS AND DISCUSSION

19A cDNA sequence

The DNA sequence of the 19A-gene open reading frame is shown in Figure 1. The primary DNA sequence was analysed using the University of Wisconsin, Genetics Computer group DNA sequence analysis suite of programs. 19A is predicted to encode a type I membrane protein 335 amino acids long with a predicted 22-residue signal sequence, a hydrophobic transmembrane region of 23 residues and a predicted cytoplasmic region of 87 residues (Figure 1). There are seven potential N-linked glycosylation sites located in the predicted extracellular region of 19A. Four tyrosine residues are present in the predicted cytoplasmic tail of 19A, and two of these are part of a tyrosine consensus motif found in other CD2 family members, including SLAM and 2B4 [2,9,18]. The predicted protein sequence of 19A shares homology with the CD2 family proteins, including CD84 (40%), SLAM (36%), 2B4 (34%) and CD2 itself (35%). Database searches have revealed that a recently submitted human genomic DNA sequence from clone RP11-404F10 on chromosome 1q23.1-24.1 (accession number AL121985) contains a novel LY9-like gene with a DNA

```

1  AATTCGGCAGCAGAGCAATATGCGTGGTTCGCCAACATGCCTCACCCCTCATCTAT  60
   M A G S P T C L T L I Y
61  ATCCTTTGGRCGCTCACAGGGTCAGCAGCCTCTGGACCCGTGAAGAGCTGGTCGGTTC  120
   I L W Q L L T G S A A S G P V K E L V G S
121 GTTGGTGGGGCCGTGACTTCCCCCTGAAGTCCAAAGTAAAGCAAGTTGACTCTATTGTC  180
   V G G A V T F P L K S K V K Q V D S I V
181 TGGACCTTCACACACACCCCTCTTGTACCATACAGCCAGAGGGGGCCTATCATAGTG  240
   W T F N T T P L V T I Q P E G G T I I V
241 ACCCAAAATCGTAATAGGGAGAGTAGACTTCCCAGATGGAGGCTACTCCCTGAAGCTC  300
   T Q N R N R E R V D F P D G G Y S L K L
301 AGCAAACTGAAGAAGAAATGACTCAGGGATCTACTATGTGGGATATACAGCTCATCACTC  360
   S K L K K N D S G I Y Y V G I Y S S S L
361 CAGCAGCCCTCCACCCAGGAGTACGTGCTGCATGTCTACGAGCACCTGTCAAAGCCTAAA  420
   Q Q P S T Q E Y V L H V Y E H L S K P K
421 GTCACCATGGGTCTGCAGGCAATAAGAATGGCACCTGTGTGACCAATCTGACATGCTGC  480
   V T M G L Q S N K N G T C V T N L T C C
481 ATGGAACATGGGAAGAGGATGTGATTATACCTGGAAGCCCTGGGGCAAGCAGCCAAT  540
   M E H G E E D V I Y T W K A L G Q A A N
541 GAGTCCCATATGGTCCATCCCTCCATCTCCTGGAGATGGGGAAGTGATATGACC  600
   E S H N G S I L P I S W R W G E S D M T
601 TTCATCTGGCTGCCAGGACCCCTGTACAGCAAACTTCTCAAGCCCATCTTGCAGG  660
   F I C V A R N F V S R N F S S P I L A R
661 AAGCTCTGTGAAGGTGCTGCTGATGACCCAGATTCCCTCATGGTCTCCTGTGTCTCTG  720
   K L C E G A A D D P D S S M V L L C L L
721 TTGGTCCCTCTGCTCAGTCTCTTGTACTGGGGCTATTTCTTGGTTTCTGAGAGA  780
   L V P L L L S L F V L G L F L W F L K R
781 GAGAGACAAGAAGAGTACATTGAAGAGAAGAAGAGAGTGGACATTTGTGGGAACTCCT  840
   E R Q E E Y I E E K K R V D I C R E T P
841 AACATATGCCCCCATCTGGAGAGAACACAGATACGACACAATCCCTCACACTAATAGA  900
   N I C P H S G E N T E Y D T I P H T N R
901 ACAATCCTAAAGGAAGTCCAGCAATACCGTTTACTCCACTGTGGAATACCGAAAAG  960
   T I L K E D P A N T V Y S T V E I P K K
961 ATGGAATAATCCCCACTCAGTGCACGATGCCAGACACCAAGGCTATTTGCCATGAG  1020
   M E N P H S L L T M P D T P R L F A Y E
1021 AATGTTATCTAGACAGCAGTGCCTGCCCTFAAGTCTCTGCTCAAAAAAACAATTTCT  1080
   N V I
1081 CGGCCCAAGAAAACATACAGG  1102

```

Figure 1 cDNA sequence of the *19A*-gene open reading frame and predicted protein sequence

The predicted signal peptide and transmembrane region are underlined. The start site and stop codon are in **bold**. Also underlined are positions of N-linked glycosylation, and the two tyrosine-containing consensus motifs in the cytoplasmic tail are double underlined.

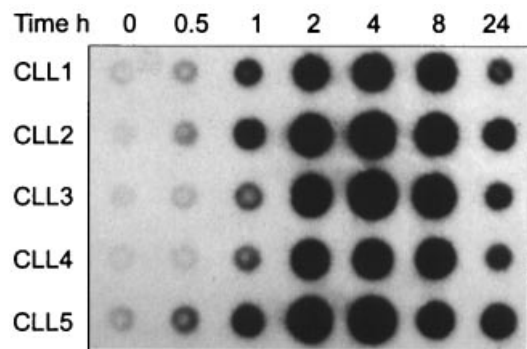


Figure 2 Time course of PMA-induced *19A* expression in different B-CLL populations

Total RNA from five different B-CLL populations stimulated with PMA (30 nM) for the times shown was dot-blotted on to nylon filters and hybridized to ^{32}P -labelled *19A* cDNA probe. Cell populations of > 95% purity were used in these experiments.

sequence virtually identical with that of the *19A* gene reported here. Interestingly, this portion of chromosome 1 also contains the 5' end of the *SLAM* gene, together with the *CD48* gene and the 5' end of *LY9* itself. This indicates that the *19A*

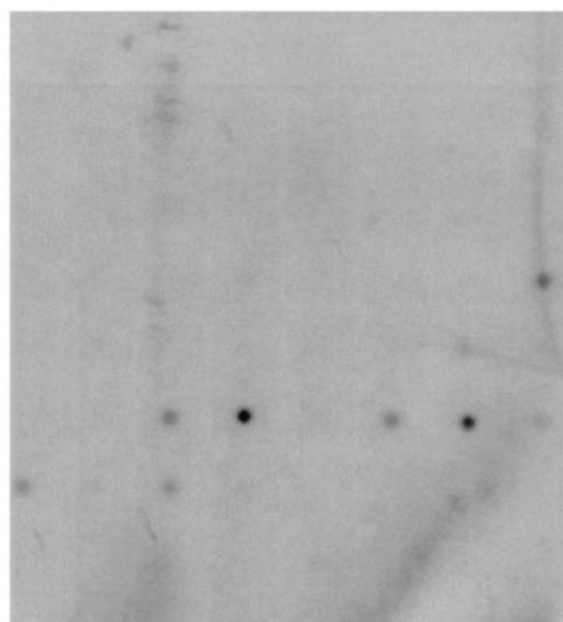


Figure 3 Expression of *19A* in different human cells and tissues

A ClonTech Human Multiple Tissue Array was hybridized to ^{32}P -labelled *19A* cDNA probe. Expression of *19A* is restricted predominantly to lymphoid tissue. Highest levels were found in the spleen and lymph nodes and lower levels in peripheral leucocytes, bone marrow, stomach, small intestine, trachea and appendix.

gene is located on chromosome 1 in close proximity to genes encoding other members of the CD2 family of membrane receptors.

19A expression in different cell types

Gene *19A* was originally cloned on the basis of its induction by PMA in primary malignant B-cells from a B-CLL patient [11]. Figure 2 shows the time course of *19A* induction in five different B-CLL populations in response to PMA (30 nM) over a 24 h period by RNA dot-blot analysis. *19A* was expressed at very low levels in unstimulated resting B-CLL cells, but it was rapidly

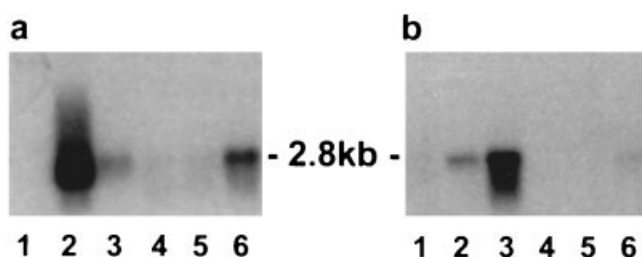


Figure 4 Northern blot showing 19A expression in different cell types in response to various stimuli

Total RNA from (a) B-CLL cells and (b) peripheral-blood T-lymphocytes and tonsillar B-lymphocytes stimulated with different agents for the times shown was isolated from cells. Different size classes of RNA were separated by formaldehyde/gel electrophoresis, blotted on to nylon filters and hybridized to ^{32}P -labelled 19A cDNA probe. Cell populations of > 95% purity were used in these experiments. (a) Lane 1, untreated cells; lane 2, stimulated with PMA (30 nM) for 3 h; lane 3, stimulated with F(ab')_2 anti- μ antibody (12.5 $\mu\text{g/ml}$) for 3 h; lane 4, stimulated with anti-CD40 antibody (G28-5, 1 $\mu\text{g/ml}$) for 3 h; lane 5, stimulated with $\text{TNF}\alpha$ (10 ng/ml) for 3 h; lane 6, stimulated with F(ab')_2 anti- μ and anti-CD40 antibody for 3 h. (b) Lane 1, untreated T-lymphocytes; lane 2, stimulated with PHA (2 $\mu\text{g/ml}$) for 3 h; lane 3, stimulated with PHA for 6 h; lane 4, untreated B-lymphocytes; lane 5, stimulated with F(ab')_2 anti- μ antibody (12.5 $\mu\text{g/ml}$) for 3 h; lane 6, stimulated with F(ab')_2 anti- μ antibody for 6 h.

induced to peak levels within 2–8 h after stimulation. Its level of expression then decreased by 24 h, but was still notably higher than basal levels of expression. A dot-blot analysis of 19A expression in a range of human tissues using a ClonTech Human Multiple Tissue Array revealed that expression of 19A appears to be confined largely to lymphoid tissue or tissues where there is a high lymphocyte content (Figure 3). Highest levels of expression were seen in the spleen and lymph node, with intermediate levels in peripheral leucocytes, bone marrow, small intestine, stomach, appendix and trachea. No detectable signal was evident for any other tissues (Figure 3). Northern blot analysis of B-lymphoid cell lines and tumour cells at various stages of lymphoid development has revealed that expression of 19A is largely confined to relatively mature lymphocytes ([11,19] and results not shown).

Multiple signalling pathways can induce 19A expression in mature B- and T-lymphocytes

We compared induced expression of 19A in purified B-CLL cells, normal tonsillar B-lymphocytes and peripheral-blood T-lymphocytes following stimulation of these cells with a number of different agents (Figure 4). In B-CLL cells, anti- μ antibody induced a low level of 19A expression, whereas $\text{TNF}\alpha$ or anti-CD40 antibody had little measurable effects on 19A expression (Figure 4a). Interestingly, the combination of anti- μ and anti-CD40 antibody added together appeared to induce 19A expression in a synergistic manner in these cells (Figure 4a). Figure 4(b) compares 19A induction in resting normal human B- (tonsillar) lymphocytes and peripheral-blood T-lymphocytes. 19A was expressed at low levels in both these cell types, but was rapidly induced in T-lymphocytes by PHA and in B-lymphocytes by anti- μ stimulation (within 3–6 h).

Molecular modelling of 19A based on CD2 crystal structure

19A is related to the CD2 family group of leucocyte differentiation proteins. Although there are no very closely related crystal structures revealed by the BLAST search, a PSI BLAST search indicated CD2 itself (PDB entry 1HNF) as a possible candidate [E (expectation) value 0.52 for the alignment of CD2 with 19A]. Preliminary examination of the alignment showed conserved positions of internal disulphide-bridge-forming cysteine, and core hydrophobic, residues. 3-D PSSM recognized 19A as a protein likely to have an immunoglobulin-like fold and provided a list of possible candidates. The CD155 molecule (PDB code: 1DGI) scored highest, with CD2 second (1HNF). However, examination of the sequence alignments reveal that not only has CD2 greater overall identity with 19A (21% compared with 10% for CD155), but also there are more instances of motif conservation in the CD2/19A alignment. The fold recognition server THREADER also identified CD2 (1HNF) as a template for modelling 19A.

The sequence of 19A was therefore aligned with CD2 according to the predictions of PSI-BLAST, 3D-PSSM and THREADER (Figure 5), and a molecular model of the predicted extracellular

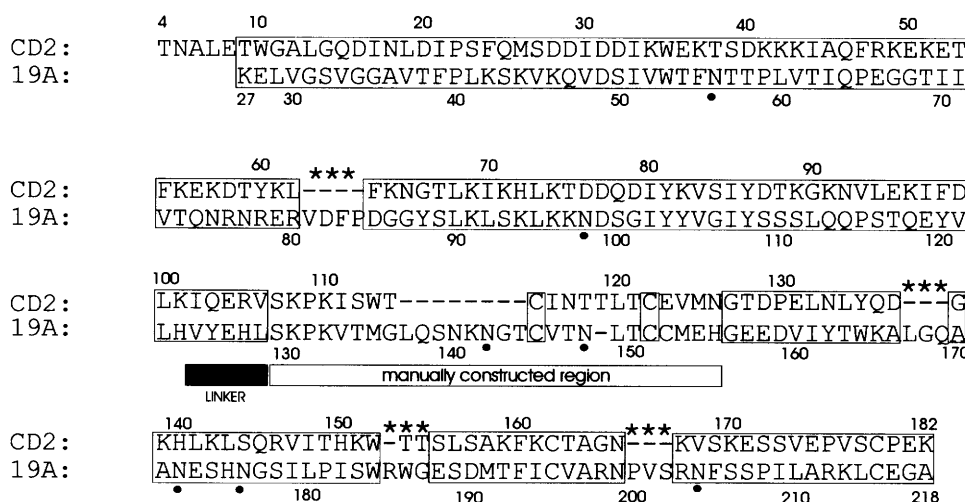


Figure 5 Structural alignment of the 19A sequence with that of CD2

Regions of sequence alignment that are boxed denote those residues for which co-ordinates for the 19A model have been assigned directly from the crystal structure of CD2 (1HNF). Regions for which co-ordinates have been determined by conformational search (GENLOOPs) are denoted with stars (★). The inter-domain linker region and manually-built region are indicated. Potential sites of N-linked glycosylation are indicated with filled circles (●) underneath the sequence.

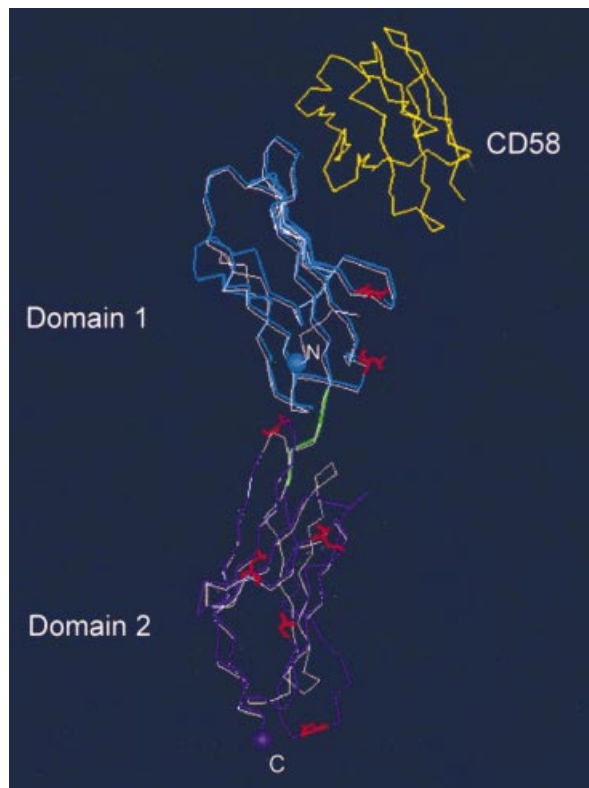


Figure 6 Modelled structure of the immunoglobulin-like domains of 19A receptor protein

The two extracellular immunoglobulin-like domains of 19A are shown in blue (N-terminal domain) and purple (C-terminal domain), superimposed upon the C α trace of the template CD2 structure in white (1HNF). The linker region is shown in green, and the seven asparagine residues that are potential sites for N-linked glycosylation are shown in red. The CD2-binding domain of CD58, located in relation to CD2 as it is found in the crystal structure of the complex (1QA9), is shown in yellow.

region of 19A, consisting of two immunoglobulin-like domains, was generated using the CD2 crystal structure (1HNF) as a template (Figure 6). There are only five insertions in the sequence of 19A relative to CD2, and one deletion [of only one residue (Figure 5)]; all occur at the surface of the modelled structure and are readily accommodated. Four of these are short extensions of existing loops, modelled using a conformational search procedure (see the Experimental section); the conformation of the eight-residue insertion is the only one that is difficult to model with any certainty. This was built manually, retaining the adjacent disulphide bridge (to Cys¹⁴⁵) and accommodating the single-residue deletion that follows (Figure 5). There is only one short insertion of four residues in domain 1, confirming that the backbone conformation is likely to be well-conserved between CD2 and 19A in this domain. The N-terminal domain 1 is thus a member of the V subset, and domain 2 a member of the C2 subset of immunoglobulin-like domains, as in CD2. The modelled structure begins at amino acid-27 downstream of the putative signal peptide of 19A (amino acids 1–22) and extends to amino acid-218 of 19A, just seven amino acids short of the predicted transmembrane region (Figure 1).

In domain 1, Trp⁵³ at the core of the domain is conserved, and all residues in the immediate vicinity are either identical with those of CD2 (Leu⁹⁰ and Val¹⁰⁵) or conservatively substituted (Tyr¹²⁰ for Phe in CD2). As in CD2, there is no intra-domain

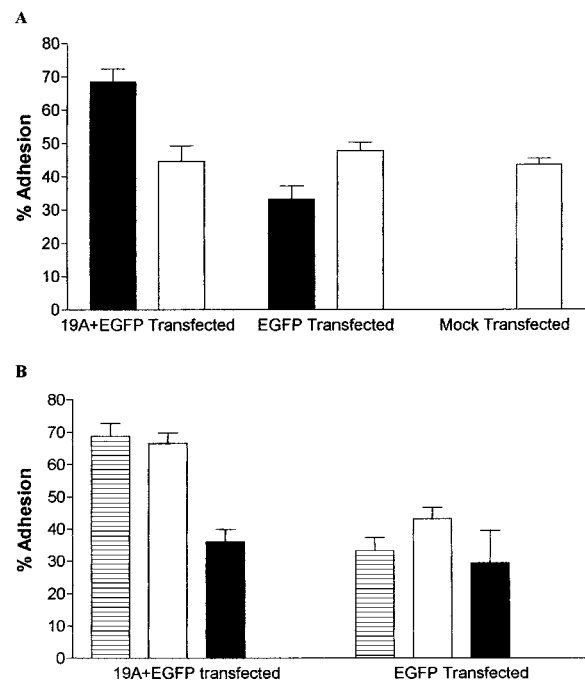


Figure 7 19A can promote cell adhesion in Daudi human B-cells

An EGFP expression construct was transfected alone or in combination with 19A cDNA, cloned into the pcDNA3 mammalian expression vector, into Daudi B cells. At 72 h after transfection, cells were assessed for levels of adhesion. At least 1000 cells were scored for each culture. Clusters of two or more adherent cells were scored as positive and the percentages of adherent fluorescent and adherent non-fluorescent cells were scored in each of the cultures. (A) Black bars represent fluorescent cells in cultures and open bars represent non-fluorescent cells. Results were analysed by an unpaired one-tailed *t*-test. A significant increase ($P < 0.001$) in cell adhesion was found in fluorescent 19A transfected cells compared with all other treatments. The results are expressed as means \pm S.E.M. for 16 independent experiments. (B) The adhesion of fluorescent 19A transfected cells compared with fluorescent EGFP-alone-transfected cells was assessed in the presence or absence of the 19A-specific antibody. Horizontally striped bars show adhesion levels of fluorescent cells in the absence of antibody. Open bars show adhesion levels in the presence of an irrelevant antibody [anti-(human IgG₁) antibody, 10 μ g/ml] and black bars represent adhesion levels of fluorescent cells in the presence of 19A-specific antibody (50 μ g/ml). 19A-specific antibody significantly inhibited adhesion of fluorescent 19A transfected cells ($P < 0.001$). Levels of adhesion in fluorescent EGFP-alone-transfected cells were significantly lower than in 19A transfected cell cultures ($P < 0.001$) and antibodies had no significant effects on levels of adhesion in EGFP-alone-transfected cell cultures. The results are expressed as means \pm S.E.M. for eight independent experiments.

disulphide bridge in domain 1. In domain 2, the two intra-domain disulphide bonds are conserved (Cys¹⁵¹–Cys¹⁹⁵; Cys¹⁴⁵–Cys²¹⁵), and all residues in the immediate vicinity of the former, in the core of the domain, are either identical with those of CD2 (Pro¹³¹) or conservatively substituted (Val¹³³, Ile¹⁶¹, Leu¹⁸⁰ in 19A, for Ile, Leu and Ile respectively in CD2). The inter-domain linker region is also identical in length between 19A and CD2, and shows some conservation (Val-Tyr-Glu-His-Leu in 19A, cf. Ile-Gln-Glu-Arg-Val in CD2), with striking conservation in the immediate flanking region of domain 2 (see Figure 5). Although there are several differences between CD2 and 19A in residues at the interface between the two domains, the sequence of 19A can be accommodated without steric clashes. It is thus possible that the relative disposition of the two domains is essentially the same as in CD2.

There is one other cysteine residue in domain 2 of 19A, namely Cys¹⁵², with no counterpart in CD2; it is predicted to be exposed on the surface of the domain. Also exposed are all seven of the potential N-linked glycosylation sites, two in domain 1 (Asn⁵⁶ and Asn⁹⁸), and five in domain 2 (Asn¹⁴², Asn¹⁴⁸, Asn¹⁷², Asn¹⁷⁶

and Asn²⁰⁴). These are shown in Figure 6; one site (Asn²⁰⁴) lies close to the inter-domain linker region.

In summary, despite the low level of sequence identity between the two proteins, when the sequence of 19A is modelled on to the structure of CD2, key core residues, and the disulphide bridges, are found to be structurally conserved; furthermore, the few insertions, the single-residue deletion, and all the potential glycosylation sites, occur at the surface. Thus 19A is not only a member of the immunoglobulin superfamily, but it is very likely to have a three-dimensional structure closely similar to that of CD2.

The crystal structure of the complex between CD2 and CD58 has been determined (PDB 1QA9, see [20]), and we have compared this with the modelled structure of 19A (see Figure 6). The backbone conformation of 19A is expected to be identical with that of CD2 in all regions that are homologous with the contact region of CD2 for CD58, since the only insertion in 19A relative to CD2 in this domain is well away from the interface (Figure 6). It is thus possible that 19A might interact with its adhesion partner in the same way, and none of the seven potential carbohydrate sites would interfere with such an interaction. This conclusion is reinforced by the striking observation that the principal buried hydrophobic residues underlying the contact surface of CD2 are all identical in 19A (Ile⁵¹, Trp⁵³, Val¹⁰⁵, Ile¹⁰⁷). Furthermore, the solvent-exposed residues in this region of 19A are dominated by hydrophobic residues (Val⁵², Val⁶¹, Val⁷², Tyr¹⁰⁴, Tyr¹⁰⁸), suggestive of a protein-protein interface. In fact the CD2-CD58 complex displays a rather unusual binding interface dominated by electrostatic interactions [20]. This charge complementarity, and relative paucity of hydrophobic interactions, appears to permit a high level of specificity within a low-affinity interaction [20,21], an observation of functional importance for this adhesion pair. However, only one of the eight charged residues that in CD2 form salt bridges to CD58 is conserved as a charged residue in 19A, which may therefore have a more conventional, hydrophobic (and perhaps higher-affinity) binding interface. If 19A does employ a homologous binding mode, albeit with interactions of a more hydrophobic nature, this would imply that the binding partner is also a member of the immunoglobulin superfamily. 19A and CD2 are clearly, if distantly, related by divergent evolution from a common ancestral molecule, and the topology of binding to an adhesion partner may also have been conserved.

19A can promote cell adhesion

As a first step in identifying possible functions of the 19A protein, we co-transfected a pcDNA3 construct of 19A together with a marker plasmid expressing EGFP into the Daudi Burkitt lymphoma cell line in order to examine whether enforced expression of 19A affected the cell-adhesion properties of the cells. Examination of transfected cultures 72 h after transfection revealed that a significantly higher proportion of EGFP-positive cells that were co-transfected with 19A were present in clusters of two or more cells compared with either EGFP-negative cells in the same population or with cells transfected with EGFP vector alone or with mock-transfected cells (Figure 7A). Furthermore, the enhanced adhesion in 19A transfected cultures was significantly inhibited by 19A-specific monoclonal antibody (Figure 7B). These data are consistent with enforced expression of 19A promoting homotypic cell adhesion. Collectively, our data suggest that, in common with other lymphocyte-specific CD2 family members that are induced by cell activation signals, the

19A protein plays a role in regulation of lymphocyte adhesion and may therefore be important in lymphocyte signalling and other functions associated with elaboration of the immune response.

This work was supported by the (U.K.) Medical Research Council and by the University of Essex Research Promotion Fund.

REFERENCES

- 1 Tangye, S. G., Phillips, J. H. and Lanier, L. L. (2000) The CD2-subset of the Ig superfamily of cell surface molecules: receptor-ligand pairs expressed by NK cells and other immune cells. *Semin. Immunol.* **12**, 149–157
- 2 Cocks, B. G., Chang, C. C. J., Carballido, J. M., Yssel, H., De Vries, J. E. and Aversa, G. (1995) A novel receptor involved in T cell. *Nature (London)* **376**, 260–263
- 3 Punnonen, J., Cocks, B. G., Carballido, J. M., Bennett, B., Peterson, D., Aversa, G. and de Vries, J. E. (1997) Soluble and membrane-bound forms of signaling lymphocytic activation molecule (SLAM) induce proliferation and Ig synthesis by activated human B lymphocytes. *J. Exp. Med.* **185**, 993–1004
- 4 Sivori, S., Parolini, S., Falco, M., Marcenaro, E., Biassoni, R., Bottino, C., Moretta, L. and Moretta, A. (2000) 2B4 functions as a co-receptor in human NK cell activation. *Eur. J. Immunol.* **30**, 787–793
- 5 Brown, M. H., Boles, K., van der Merwe, P. A., Kumar, V., Mathew, P. A. and Barclay, A. N. (1998) 2B4, the natural killer and T cell immunoglobulin superfamily surface protein, is a ligand for CD48. *J. Exp. Med.* **188**, 2083–2090
- 6 Latchman, Y., McKay, P. F. and Reiser, H. (1998) Cutting edge: identification of the 2B4 molecule as a counter-receptor for CD48. *J. Immunol.* **161**, 5809–5812
- 7 Sayos, J., Wu, C., Morra, M., Wang, N., Zhang, X., Allen, D., Van Schaik, S., Notarangelo, L., Geha, R., Roncarolo, M. G. et al. (1998) The X-linked lymphoproliferative-disease gene product SAP regulates signals induced through the co-receptor SLAM. *Nature (London)* **395**, 462–469
- 8 Schatzle, J. D., Sheu, S., Stepp, S. E., Mathew, P. A., Bennett, M. and Kumar, V. (1999) Characterization of inhibitory and stimulatory forms of the murine natural killer cell receptor 2B4. *Proc. Natl. Acad. Sci. U.S.A.* **96**, 3870–3875
- 9 Nakajima, H. and Colonna, M. (2000) 2B4: an NK cell activating receptor with unique specificity and signal transduction mechanism. *Hum. Immunol.* **61**, 39–43
- 10 Murphy, J. J., Newton, J. S. and Norton, J. D. (1997) Early response genes and B cell activation. In *Lymphocyte Signalling*, pp. 183–202, John Wiley and Sons, Chichester
- 11 Murphy, J. J. and Norton, J. D. (1990) Cell type specific early response gene expression during plasmacytoid differentiation of human B lymphocytic leukaemia cells. *Biochim. Biophys. Acta* **1049**, 262–271
- 12 Norton, J. D. (2000) ID helix-loop-helix proteins in cell growth, differentiation and tumorigenesis. *J. Cell Sci.* **113**, 3897–3905
- 13 Davis, S. J., Davies, E. A. and Van der Merwe, P. A. (1995) Mutational analysis of the epitopes recognized by anti-(rat) CD2 and anti-(rat) CD48 monoclonal antibodies. *Biochem. Soc. Trans.* **23**, 188–194
- 14 Altschul, S. F., Madden, T. L., Schaffer, A. A., Zhang, J. H., Zhang, Z., Miller, W. and Lipman, D. J. (1997) Gapped BLAST and PSI-BLAST: a new generation of protein database search programs. *Nucleic Acids Res.* **25**, 3389–3402
- 15 Kelley, L. A., MacCallum, R. M. and Sternberg, M. J. E. (2000) Enhanced genome annotation using structural profiles in the program 3D-PSSM. *J. Mol. Biol.* **299**, 501–522
- 16 Fischer, D. and Eisenberg, D. (1996) Protein fold recognition using sequence-derived predictions. *Protein Sci.* **5**, 947–955
- 17 Laskowski, R., MacArthur, M., Moss, D. and Thornton, J. M. (1993) PROCHECK — a program to check the stereochemical quality of protein structures. *J. Appl. Crystallogr.* **26**, 283–291
- 18 Boles, K. S., Nakajima, H., Colonna, M., Chuang, S. S., Stepp, S. E., Bennett, M., Kumar, V. and Mathew, P. A. (1999) Molecular characterization of a novel human natural killer cell receptor homologous to mouse 2B4. *Tissue Antigens* **54**, 27–34
- 19 Green, R. M., Murphy, J. J. and Norton, J. D. (1991) Use of cDNA probes for typing cells of B-lymphoid lineage — application of early response genes to the analysis of mature B cell malignancies. *Leukemia Lymphoma* **3**, 325–329
- 20 Wang, J., Smolyar, A., Tan, K. M., Liu, J., Kim, M. Y., Sun, Z. J., Wagner, G. and Reinherz, E. L. (1999) Structure of a heterophilic adhesion complex between the human CD2 and CD58 (LFA-3) counter-receptors. *Cell (Cambridge, Mass.)* **97**, 791–803
- 21 Davis, S. J., Ikemizu, S., Wild, M. K. and van der Merwe, P. A. (1998) CD2 and the nature of protein interactions mediating cell-cell recognition. *Immunol. Rev.* **163**, 217–236